A Comparative Study of Multi-objective Metaheuristics for Solving Hyperparameter Tuning of Terminal Sliding Mode Controller

Alireza Beigi
School of Mechatronic Systems Engineering
Simon Fraser University
Surrey, B.C. Canada V3T 0A3
alireza_beigi@sfu.ca

Krishna Vijayaraghavan
School of Mechatronic Systems Engineering
Simon Fraser University
Surrey, B.C. Canada V3T 0A3
krishna@sfu.ca

Gary Wang
School of Mechatronic Systems Engineering
Simon Fraser University
Surrey, B.C. Canada V3T 0A3
gary_wang@sfu.ca

***Abstract*—Multi-objective optimization plays a vital role in many applications of control and engineering problems. One of them is tuning the hyperparameters of the controller system, which is focused on identifying the best hyperparameters to satisfy desired aims such as reducing error, efficient energy consumption, and so on. These setting are included in a multi-objective optimization problem to find the proper controller hyperparameters. In this paper, we first develop a new terminal sliding mode controller schema for a single-input single-output system in presence of external disturbances and provide the Lyapunov proof to guarantee the stability of the system. Then, we study the hyperparameter optimization of the proposed controller with different maximum function evaluation numbers. Finally, the simulation results for a pendulum-driven spherical robot are presented to illustrate the effectiveness and superiority of the proposed control technique.**

Keywords—Terminal Sliding mode, Hyperparameter Tuning, Metaheuristics algorithms, Multi-Objective Optimization

I. Introduction

Tuning the hyperparameters of controllers is one of the challenging problems for engineers when it is required to deal with complex plants. Therefore, there are several strategies to overcome this problem [1]. One of them is the application of multi-objective optimization to solve the problem of hyperparameter selection for terminal sliding mode controllers.

The application of Metaheuristic Optimization for tuning parameters of controllers has been widely popular. Janprom et al. [2] present an optimization-based approach for tuning gains of proportional integral derivative (PID) controller to control the temperature and relative humidity of a comfortable room. In this study, the ant colony optimization (ACO), and symbiotic organism search (SOS) are used to identify the gains of the PID controller. Chaib et al. [3] propose a novel fractional order PID controller tuned by a metaheuristic Bat algorithm to stabilize the power system. Roeva et al. [4] present a metaheuristic-based optimal tuning of a PID controller. In this research, Genetic Algorithms (GA), Simulated Annealing (SA), and Tabu Search (TS) are provided and it is shown that the proposed metaheuristic algorithms can improve the result and performance of traditional methods significantly.

This article is organized as follows. Section II presents the terminal sliding mode control with a disturbance observer and the stability of the controller schema is proven by the Lyapunov method. Then, the multi-objective optimization problem is introduced in Section III. Also, four different multi-objective optimizations are presented in this section. Section IV presents the simulation of the proposed algorithm and discusses the experimental tests. Finally, Section V concludes this paper.

II. Controller Design

Let us consider SISO nonlinear dynamical system

$$\dot{x}_i = x_{i+1},\ i = 1,2,\dots,n-1 \tag{1}$$

$$\dot{x}_n = f(x) + g(x)u + d \tag{2}$$

$$y = x_1 \tag{3}$$

where $x = [x_1, x_2, \dots, x_n]$ denotes the vector of measurable state of the nonlinear system, $g(x) \in \mathbb{R}$ and $f(x) \in \mathbb{R}$ are nonlinear functions and are considered as known functions, $u \in \mathbb{R}$ is the input controller, $y \in \mathbb{R}$ denotes the output of the system. In this system, the external disturbances are imposed through $d \in \mathbb{R}$.

Lemma 1: Consider the continuous function $V(t)$ which is positive definite and satisfies the following inequality:

$$\dot{V}(t) + \alpha V(t) + \lambda V^{\lambda} \leq 0 \tag{4}$$

for $\forall t > t_0$. Therefore, one can conclude that $V(t)$ converges to its equilibrium point infinite time t_s which t_s can be derived as follows:

$$t_s \leq t_0 + \frac{1}{\alpha(1+\gamma)} \ln \frac{(\alpha V^{1-\gamma}(t_0) + \lambda)}{\lambda} \tag{5}$$

where α and λ are positive and $0 < \gamma < 1$.

In this paper, the aim is to design the chatter-free disturbance-observer-based terminal sliding mode, tracking controller. In this regard, the proposed controller should ensure that the system output y will converge to the desired system output y_d in finite time.

Assumption 1 (Man and Yu [1])*:* the desired system output $y_d(t)$ is bounded such that $\|y_d(t)\| \leq y_d^{max}$

To design the terminal sliding mode observer with finite time convergency, the auxiliary variable z is defined such that:

$$\dot{z} = -ks - \beta \tanh(s) - \epsilon s^{p_0/q_0} - |f(x)| \tanh(s) + g(x)u \tag{6}$$

where $s = z - x_n$ and $0 < p_0 < q_0$, which are odds, and Design parameters k, β, and ϵ are positive and $\beta > |d|$. Therefore, the disturbance observer can be designed as follow:

$$\hat{d} = -ks - \beta \tanh(s) - \epsilon s^{p_0/q_0} - |f(x)| \tanh(s) - f(x) \quad (7)$$

Instead of using $sign(.)$, the $\tanh(.)$ Is employed to reduce the fast-changing of input controller through time. Therefore, this smoothness in function can reduce the chattering phenomenon for the input controller. By differentiating $s = z - x_n$, and (2), $\dot{s}$ can be given

$$\begin{aligned} \dot{s} = \dot{z} - \dot{x}_n = &-ks - \beta \tanh(s) - \epsilon s^{p_0/q_0} \\ &- |f(x)| \tanh(s) + g(x)u - f(x) \\ &- g(x)u - d \end{aligned} \quad (8)$$

Theorem 1 (Tee and Ge [5]). Assuming that the uncertain SISO nonlinear system (1)-(3), the terminal sliding mode disturbance observer is determined as (6)-(8). Hence, the disturbance approximation error of the proposed terminal sliding mode disturbance observer is convergent in finite time.

Proof. Let us consider the Lyapunov function as follow

$$V_0 = \frac{1}{2} s^2 \quad (9)$$

Differentiating from (9) yields

$$\begin{aligned} \dot{V}_0 = s\dot{s} = s\big(&-ks - \beta \tanh(s) - \epsilon s^{p_0/q_0} \\ &- |f(x)| \tanh(s) - f(x) - d\big) \\ &\leq -ks^2 - \beta s \tanh s - \epsilon s s^{p_0/q_0} \\ &+ |s||d| \leq -ks^2 - \epsilon s s^{p_0/q_0} \\ &\leq -2kV_0 - 2^{\frac{p_0+q_0}{2q_0}} \epsilon V_0^{\frac{p_0+q_0}{2q_0}} \end{aligned} \quad (10)$$

Using (1)-(3) and (6)-(8), one can obtain

$$\begin{aligned} \tilde{d} = \hat{d} - d = &-ks - \beta \tanh(s) - \epsilon s^{p_0/q_0} \\ &- |f(x)| \tanh(s) - f(x) - \dot{x}_n \\ &+ f(x) + g(x)u \\ &= -ks - \beta \tanh(s) - \epsilon s^{p_0/q_0} \\ &- |f(x)| \tanh(s) - \dot{x}_n + g(x)u \\ &= \dot{z} - \dot{x}_n \end{aligned} \quad (11)$$

Due to *Lemma 1* and (10), one can obtain that the variable s converges to the equilibrium point in the finite time. According to the finite time convergency of the s, it can be concluded that the disturbance observer $\hat{d}$ converges to the external disturbance and the error of disturbance estimation converges to zero in finite time. This can prove the statement.

To introduce the tracking controller method for this case and by assuming the availability of all states, the terminal sliding mode (TSMC) tracking controller is designed. First, s_1 is introduced.

$$s_1 = y - y_d \quad (12)$$

The n order of differentiating s_1, we have

$$s_1^{(n)} = y^{(n)} - y_d^{(n)} \quad (13)$$

Let us consider (13), the iterative process of TSMC of the nonlinear systems (1)-(3) can be given as [6]

$$\begin{aligned} &s_2 = \dot{s}_1 + \alpha_1 s_1 + \beta_1 s_1^{\frac{p_1}{q_1}} \\ &s_3 = \dot{s}_2 + \alpha_2 s_2 + \beta_2 s_2^{p_2/q_2} \\ &\dots \\ &s_n = \dot{s}_{n-1} + \alpha_{n-1} s_{n-1} + \beta_{n-1} s_{n-1}^{p_{n-1}/q_{n-1}} + s \end{aligned} \quad (14)$$

where α_i and β_i are positive and we have $0 < p_i < q_i$ which are odd integer numbers. These constraints will be imposed for the optimization problem. By expanding the recursive procedure of (14), one can obtain

$$\dot{s}_n = s_1^{(n)} + \sum_{j=1}^{n-1} \alpha_j s_j^{n-j} + \sum_{j=1}^{n-1} \beta_j \frac{d^{(n-j)}}{dt^{(n-j)}} s_j^{p_j/q_j} + \dot{s} \quad (15)$$

Thus, according to (1)-(3) and (13), we obtain

$$\begin{aligned} \dot{s}_n = \dot{x}_n - y_d^{(n)} + \sum_{j=1}^{n-1} \alpha_j s_j^{n-j} + \sum_{j=1}^{n-1} \beta_j \frac{d^{(n-j)}}{dt^{(n-j)}} s_j^{p_j/q_j} \\ + \dot{s} \\ = f(x) + v_r + D - y_d^{(n)} \\ + \sum_{j=1}^{n-1} \alpha_j s_j^{n-j} \\ + \sum_{j=1}^{n-1} \beta_j \frac{d^{(n-j)}}{dt^{(n-j)}} s_j^{p_j/q_j} + \dot{s} \end{aligned} \quad (16)$$

Therefore, the disturbance-observer-based terminal sliding mode tracking control is developed as

$$u = -\frac{u_0}{g(x)} \quad (18)$$

$$\begin{aligned} u_0 = f(x) - y_d^{(n)} + \sum_{j=1}^{n-1} \alpha_j s_j^{n-j} + \sum_{j=1}^{n-1} \beta_j \frac{d^{(n-j)}}{dt^{(n-j)}} s_j^{\frac{p_j}{q_j}} + \hat{d} \\ + \delta s_n + \mu s_n^{p_n/q_n} \end{aligned}$$

For the second order system, $n = 2$. Therefore, if we assume that $g(x) \neq 0$, therefore, the input controller for the second-order system can be derived as follow

$$u = -\frac{u_0}{g(x)} \quad (19)$$

$$\begin{aligned} u_0 = f(x) - \ddot{y}_d + \alpha_1(\dot{s}_1) + \beta_1 \left(\frac{d}{dt} \left(s_1^{\frac{p_1}{q_1}} \right) \right) + \hat{d} + \delta s_2 \\ + \mu s_2^{p_2/q_2} \end{aligned}$$

where δ and μ are positive. The stability proof of this controller is summarized in the following theorem.

Theorem 2. Let us consider system (1)-(3), as a general uncertain nonlinear system in the presence of disturbances, and assuming the system is known, the proposed controller with sliding mode disturbance observer is developed as (6) and (7). B considering the proposed controller, the convergency of the input controller in finite time is proved.

Proof. Using (17), (18) can be rewritten

$$\begin{aligned} \dot{s}_n = -\delta s_n - \mu |s|^{\frac{p_0}{q_0}} + d - \hat{d} + \dot{s} \\ = -\delta s_n - \mu s_n^{p_n/q_n} + \tilde{d} + \dot{s} \end{aligned} \quad (20)$$

Substituting (11) into (20), one can obtain

$$\dot{s}_n = -\delta s_n - \mu s_n^{p_n/q_n} \quad (21)$$

Assuming the Lyapunov function candidate

$$V = \frac{1}{2} s_n^2 \quad (22)$$

Using (10), we have the time derivative of V as

$$\dot{V} \le -\delta s_n^2 - \mu s_n^{\frac{p_n}{q_n}+1} \le -2\delta V - \mu 2^{\frac{p_n+q_n}{2q_n}} \epsilon V^{\frac{p_n+q_n}{2q_n}} \tag{22}$$

Due to *Lemma 1* and (10), one can conclude all the closed-loop signals will converge to the equilibrium point in the finite time. This can prove the statement.

Remark 1. In the proposed input controller, several hyperparameters should be designed by the researcher. In this regard, we evaluate four different optimization functions to identify the hyperparameters based on developing different objectives. In the next section, first, the optimization problem is introduced, and the next four benchmarks of multi-objective optimization algorithms are provided.

III. Hyperparameter Optimization

In the previous section, the terminal sliding mode tracking control has been presented. In this section, we implement four different multi-objective optimizations to select the hyperparameters of the proposed controller. The optimization problem is designed as follows:

$$\min_{\theta} \begin{cases} f_1 = \int_0^T |\dot{u} - \dot{\bar{u}}|\, dt \\ f_2 = \int_0^T |s_1|\, dt \\ f_3 = \int_0^T |s_2|\, dt \quad \theta_i > 0 \\ f_4 = \int_0^T t s_1^2\, dt \\ f_5 = \int_0^T |u|\, dt \end{cases} \tag{23}$$

where f_1 states the chattering measurement based on [7], [8], and shows the difference between the input controller and the nominal value of the input controller. f_2 and f_3 denote the integration of absolute value of sliding surfaces, respectively. Then, f_4 is the integral of time multiplied by squared error [9], [10] and f_5 is the integral of the absolute value of the input controller. This fitness function is considered to minimize the absolute value of dissipated energy of actuators. The optimization constraints are obtained based on the limitation of designed controller parameters which is explained in (14). According to (7) and (19), this optimization problem has six hyperparameter variables as follows

$$\theta = [\alpha_1, \beta_1, \delta, \mu, \gamma, k] \tag{24}$$

$$\theta_i > 0$$

$$\beta_1 > |d|$$

Here, the objective functions, constraints, and variables are defined. To optimize these variables, four benchmarking multi-objective optimization algorithms are considered. In this study, we use Platypus [11] library to compare the results of these algorithms summarized as follows:

- Non-dominated Sorting Genetic Algorithm III (NSGA-III) [12].
- Non-dominated Sorting Genetic Algorithm II (NSGA-II) [13].
- Particle swarm optimization-based multi-objective optimization using crowding, mutation, and ϵ −dominance (OMOPSO) [14].
- Speed-constrained Multi-objective Particle Swarm Optimization (SMPSO) [15].

In what follows, these algorithms are briefly introduced.

A. The Non-Dominated Sorting Genetic Algorithm II (NSGA-II)

In this algorithm, the individuals are divided into different classes based on their dominance. Therefore, the first class is assigned to the non-dominated individuals and the second and next classes are determined to the individuals which are dominated by the others. When each iteration finishes, the distances among the individuals are computed. The criteria for these distances are known as crowding distances, for sorting the individuals. The flowchart of the algorithm is illustrated in Fig. 1.

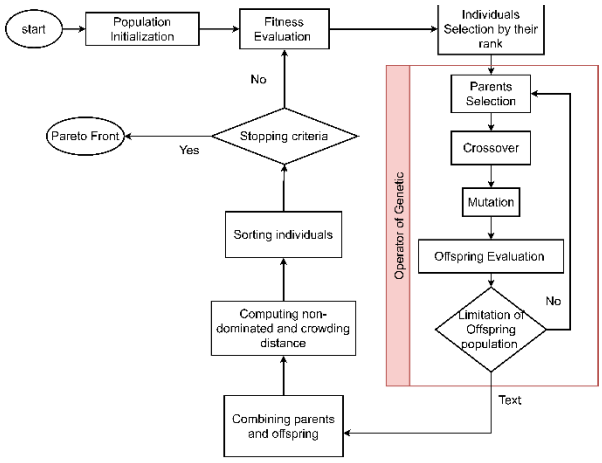

Fig. 1. Flowchart of NSGA-II Algorithm for multi-objective optimization

B. The Non-Dominated Sorting Genetic Algorithm III (NSGA-III)

NSGA-III is a new version of NSGA-II proposed by Deb and Jain [12]. In this algorithm, there is a hyper-plane to enhance the diversity feature of the population. This hyper-plane is generated by a group of predefined points. In addition, the operator is selected adaptively, therefore, this algorithm has a better performance when it is required to deal with a large number of objective functions.

C. Optimized Multi-Objective Particle Swarm Optimization (OMOPSO)

One of the efficient versions of multi-objective Particle Swarm Optimization (MOPSO) is OMOPSO which is presented by Reyes-Sierra et al [14]. In this algorithm, to regulate the number of particles, the leaders and crowding distance is identified based on non-dominated particles of the Pareto front. In each iteration, a global leader is identified, then for this generation, the other leaders are excluded from the global leaders. In addition, in this algorithm, there are different mutation operators for each group of population. The flowchart of the algorithm is illustrated in Fig. 2.

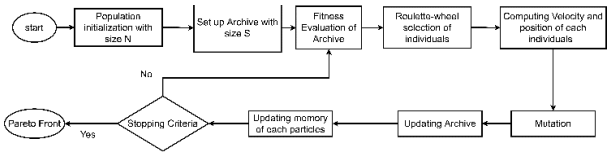

Fig. 2. Flowchart of OMOPSO Algorithm for multi-objective optimization

D. Speed-Constrained Multi-Objective Particle Swarm Optimization (SMPSO)

Another version of MOPSO is SMPSO which is proposed by Nebro et al [15]. In this algorithm, to reduce the acceleration of high-speed particles, a mechanism for speed constraint is utilized [16]. This coefficient is presented as follows

$$K = \frac{2}{2 - P_\gamma - \sqrt{P_\gamma^2 - 4P_\gamma}} \tag{25}$$

where

$$P_\gamma = \begin{cases} c_1 + c_2 & if\ c_1 + c_2 > 4 \\ 1 & if\ c_1 + c_2 \le 4 \end{cases} \tag{26}$$

In which c_1 and c_1 denote the control parameters of personal and global best particles. Then, the velocity of the i particle in generation t can be derived with this formula.

$$\vec{v}_i(t) = K\left[w.\vec{v}_i(t-1) + C_1.r_1.\left(\vec{x}_{pi}(t) - \vec{x}_i(t)\right) + C_2.r_2.\left(\vec{x}_{gi}(t) - \vec{x}_i(t)\right)\right] \tag{27}$$

In this equation, r_1 and r_2 are two random variables in the range $[0,1]$, and w is the inertia weight of the particle for controlling the trade-off between the experience and the new update. Then, the $\vec{v}_i(t)$ is bounded between upper and lower limits.

IV. Numerical Simulation

In this section, a simulation study of the proposed algorithm is given to compare different types of Multi-Objective Optimization for parameter tuning of terminal sliding mode controllers.

Consider a pendulum-driven spherical robot [17] system as

$$\begin{aligned} \dot{x}_1 &= x_2 \\ \dot{x}_2 &= -\frac{m_p^2\rho^2 r^2 \sin(x_1)\cos(x_1)\,x_2^2}{I_c m_p r^2 + m_p^2\rho^2 r^2 \sin^2(x_1)} \\ &\quad + \frac{M g r_G \sin(x_1)\left(I_c + m_p\rho^2\right)}{I_c m_p r^2 + m_p^2\rho^2 r^2 \sin^2(x_1)} \\ &\quad + \frac{I_c + m_p\rho^2 - m_p\rho r\cos x_1}{I_c m_p r^2 + m_p^2\rho^2 r^2 \sin^2(x_1)}u \\ &\quad + d \\ y &= x_1 \end{aligned} \tag{28}$$

Where $x_1 = \theta$ denoting the Instantaneous angle of the pendulum and $d = 0.05 + 0.05\sin\left(\frac{\pi}{3}t + \frac{\pi}{6}\right)$(it means that $\beta > 0.1 \ge |d|$). The system's parameters are considered as $m_p = 0.639\,kg$, $M = 1.139\,kg$, $\rho = 0.2\,m$, $r_G = 0.101\,m$ and $I_c = 0.05m^4$.

This system is demonstrated in Fig. 3.

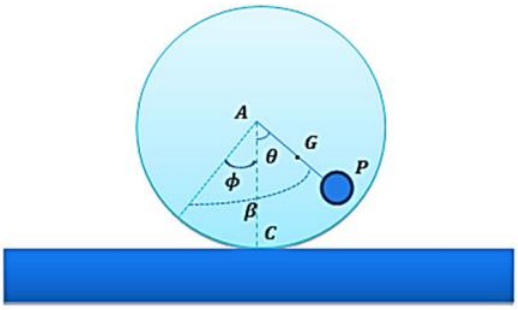

Fig. 3. A pendulum-driven spherical robot system on a flat surface

The initial condition for this system is considered $[x_1(0), x_2(0)] = [0.1, 0.0]$ and the sampling time is chosen 0.01.

In this simulation, the desired output is taken as $y_d = 0.4\sin(t)$ and the controller parameters are taken $p_0 = p_1 = p_2 = 3$ and $q_0 = q_1 = q_2 = 5$. For this tracking problem, the input controller and disturbance observer are designed based on (19) and (7). To achieve the best result concerning the minimum in chattering, error, and input controller, the optimization problem (23) is developed to choose the designing parameters in (7) and (19). This optimization problem is solved by four benchmarking algorithms including NSGA-II, NSGA-III, OMOPSO, and SMPSO with different maximum function evaluations.

The initialization of each algorithm is summarized in Table I. In addition, the lower bound and upper bound of the variables are included in Table 2.

TABLE I. Parameters Of Optimizarts

NSGA-II Parameters					
Selection	***Mutation***	***Recombination***			***Population size***
Binary tournament	$pm = 1/L$ Polonyminal	$pc = 0.9$			100
OMOPSO Parameters					
epsilons	***Swarm size***	***Leader size***	***Mutation probability***	***Maximum perturbation***	***Maximum iterations***
0.05	100	100	0.1	0.5	100
c_1	c_2	r_1	r_2		w
$\mathcal{U}_{[1.5,2]}$	$\mathcal{U}_{[1.5,2]}$	$\mathcal{U}_{[0,1]}$	$\mathcal{U}_{[0,1]}$		$\mathcal{U}_{[0.1,0.5]}$
SMPSO Parameters					
Swarm size	***Leader size***	***Mutation probability***	***Maximum perturbation***	***Maximum iterations***	
100	100	0.1	0.5	100	
c_1	c_2	r_1	r_2	w	
$\mathcal{U}_{[1.5,2.5]}$	$\mathcal{U}_{[1.5,2.5]}$	$\mathcal{U}_{[0,1]}$	$\mathcal{U}_{[0,1]}$	$\mathcal{U}_{[0.1,0.1]}$	
NSGA-III Parameters					
Selection	***Mutation***	***Recombination***			***Divisions outer***
Binary tournament	$pm = 1/L$ Polonyminal	$pc = 0.9$			12

TABLE II. RANGE OF VARIABLES

	α_1	β_1	δ	μ	γ	k
Lower Bound	0.1	0.1	0.1	0.1	0.1	0.1
Upper Bound	100	10	100	10	100	10

To create a Degree of Freedom for strategy making, this optimization uses no prioritization. Therefore, the non-dominated solution is included in the results and the hyper-plane of the Pareto Front. With this strategy, the algorithm has more options to select the best value of Pareto Front and reach the global optimum.

The optimization schema is evaluated with the different maximum number of function evaluations. The best result for the optimization problem is demonstrated in Table III-VI and Fig. 4 and 5. As one can see in this figure, first the maximum number of function evaluations is set to 50 and for the best result of tunned hyperparameters, the simulation is repeated, and Figs. 4(A1-A3) are obtained, and different optimization algorithms are compared to each other in Figs. 5(A1-A5) and Table IV. Next, the maximum number of function evaluations is set to 200 for the best result of tunned hyperparameters the simulation is repeated, and Figs. 4(B1-B3) are obtained, different optimization algorithms are compared to each other in Figs. 5(B1-B5) and Table V. Finally, the maximum number of function evaluations is set to 500 for the best result of tunned hyperparameters the simulation is repeated, and Figs. 4(C1-C3) are obtained, and different optimization algorithms are compared to each other in Figs. 5(C1-C5) and Table VI.

The execution time of each algorithm with different maximum number of function evaluation is shown in Table III. Regarding running time, NSGA-II has a better performance in average result. Instead of NSGA-III, all algorithms have a good result in execution time.

In next subsection, we compare the result of each optimization algorithm for each stage.

A. *Number of function Evaluation = 50*

In this stage, chattering is not sorted out in some algorithms and it can be seen in Fig. 4(A3). However, NSGA-III has better performance rather than the others regarding chattering. The superiority of this algorithm is shown in Fig 5(A1-A5) because this algorithm has a better average of objective functions with respect to the others. In addition, this superiority is highlighted in Table IV.

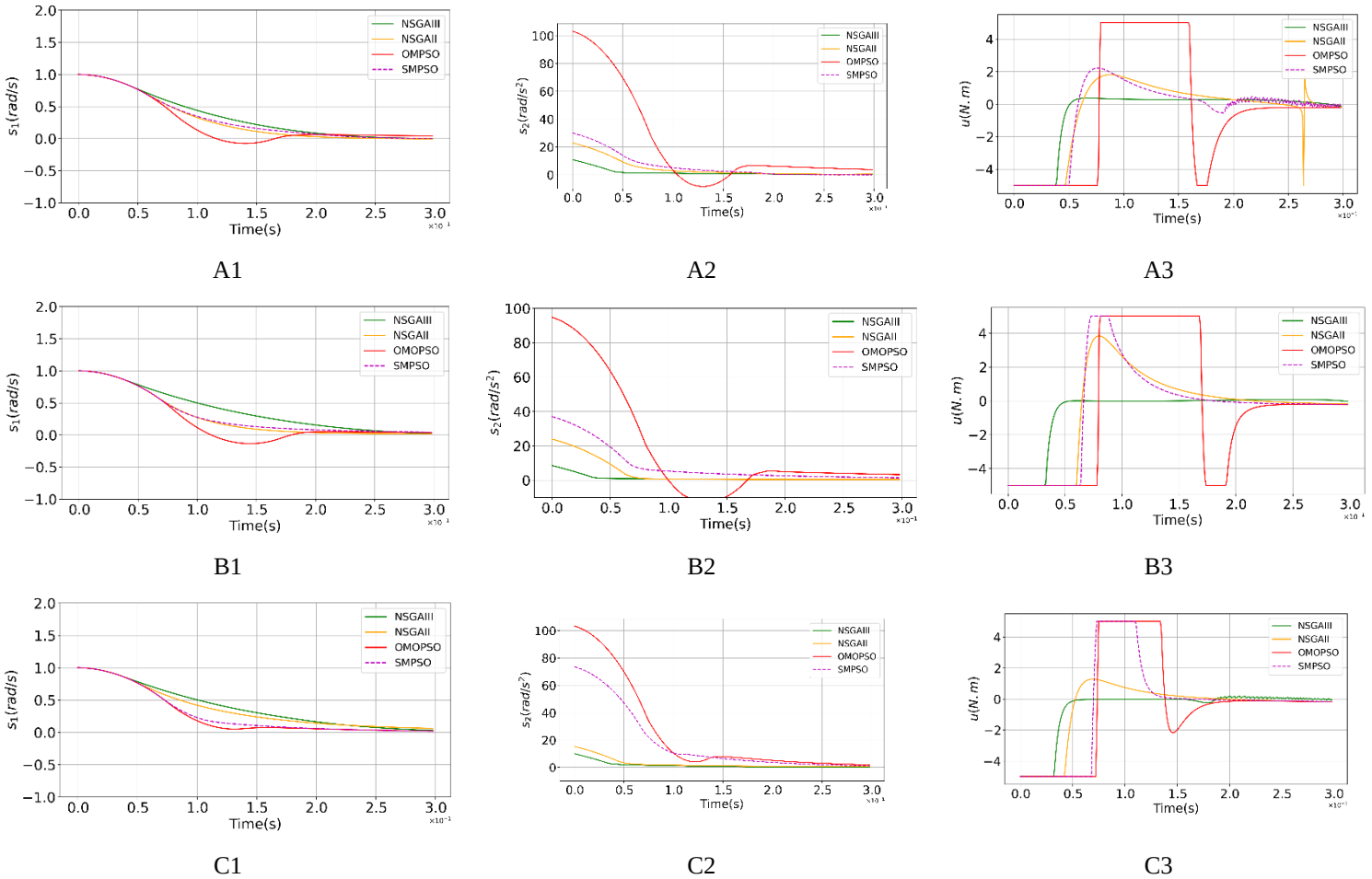

Fig. 4. Sliding surfaces and control input of the best-tuned terminal sliding mode controller for a pendulum-driven spherical robot system. The tuning is performed with four optimization algorithms including NSGA-III, NSGA-II, OMOPSO, and SMPSO with maximum function evaluation = 50 (A1-A3), maximum function evaluation = 200 (B1-B3), and maximum function evaluation = 500 (C1-C3)

B. Number of function Evaluation = 200

As one can see in Fig. 4(B3), the chattering is sorted out but the problem of high value for the input controller has remained. In these plots, the NSGA-III has better performance rather than the others regarding chattering. The superiority of this algorithm is shown in Fig 5(B1-B5) because this algorithm has a better average of objective functions to the others. In addition, this superiority is highlighted in Table V.

C. Number of function Evaluation = 500

By increasing the limit, all algorithms can find better results, regarding optimality in input controller and chattering phenomenon. This fact is shown in Fig. 4(C3). In addition, regarding tracking error, the NSGA-II has a better result rather than the others. In addition, NSGA-II could gain a better performance regarding the minimization of objective functions, and this fact is illustrated in Fig. 5(C1-C5) and highlighted in Table VI.

TABLE III. EXECUTION TIME OF OPTIMIZATION ALGORITHMS

Algorithm	**Running Time (s)**		
	Function evaluations = 50	***Function evaluations = 200***	***Function evaluations = 500***
SMPSO	5.24554880	11.7175694	**27.0013235**
NSGAII	**4.97656430**	10.5482522	28.6823616
NSGAIII	118.9245700	100.5715414	172.6694464
OMOPSO	5.65093240	**10.3312371**	27.8997733

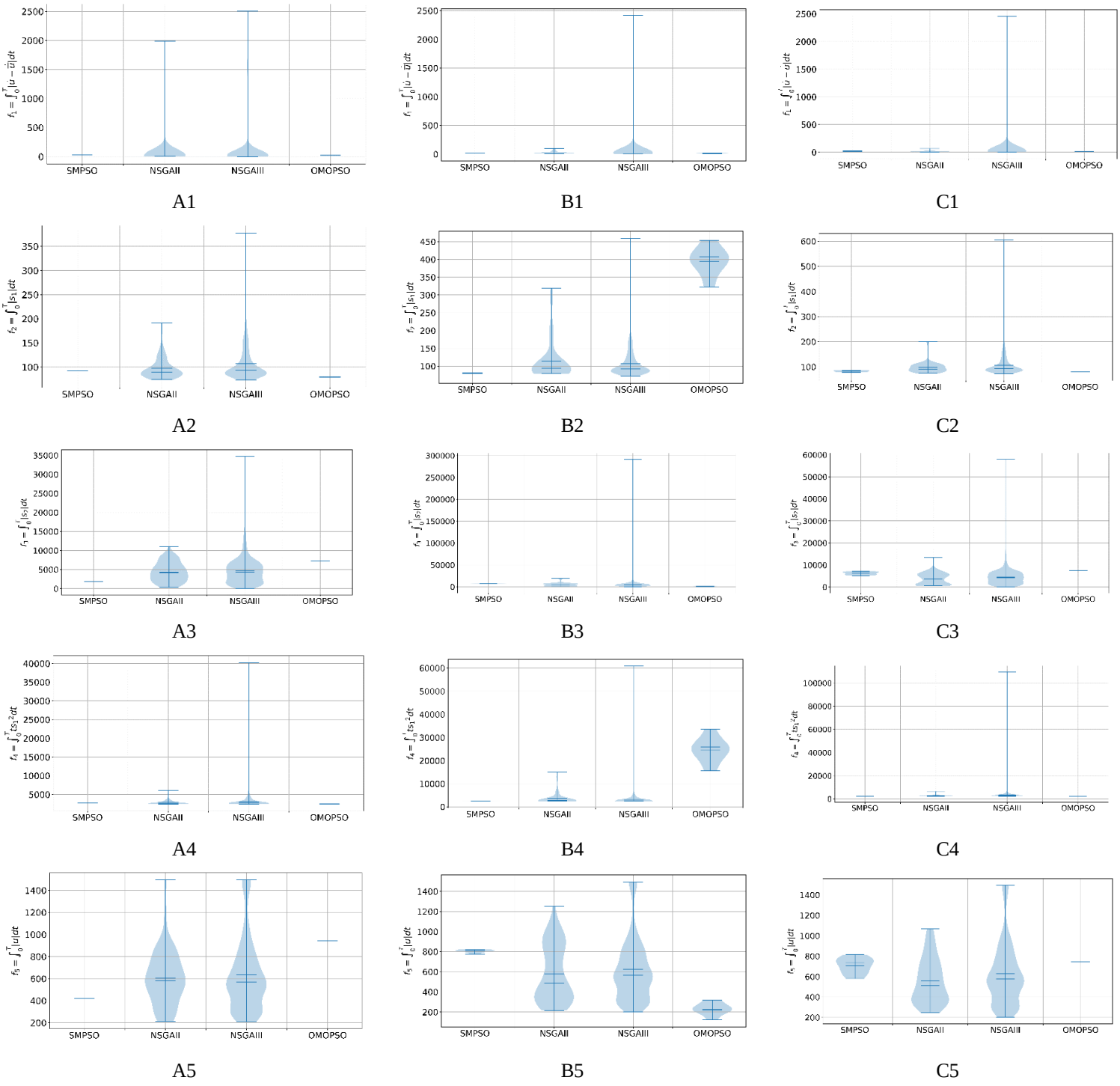

Fig. 5. Objective functions comparison of four optimization algorithm including SMPSO, NSGA-II, NSGA-III and OMOPSO with maximum function evaluation = 50 (A1-A5), maximum function evaluation = 200 (B1-B5) and maximum function evaluation = 500 (C1-C5)

TABLE IV. COMPARISON OF DIFFERENT ALGORITHM FOR TUNNING HYPERPARAMETERS OF NONSINGULAR TERMINAL SLIDING MODE CONTROLLER WITH 50 LIMITS FOR FUNCTION EVALUATION

Tuned Hyperparameters of Nonsingular Terminal Sliding Mode Controller with 50 limits for function evaluation						
SMPSO	α_1	β_1	δ	μ	γ	k
	20.45401706	9.935067	33.941272	6.265627	80.618261	7.99692
	$f_1 = \int_0^T \lvert\dot{u} - \ddot{\bar{u}}\rvert dt$	$f_2 = \int_0^T \lvert s_1\rvert dt$	$f_3 = \int_0^T \lvert s_2\rvert dt$	$f_4 = \int_0^T t s_1^2 dt$	$f_5 = \int_0^T \lvert u\rvert dt$	Feasibility
	30.12081229	92.71826475	1843.41556395	2751.80613499	420.11904768	Yes
NSGAII	α_1	β_1	δ	μ	γ	k
	18.255818	5.04240	24.410746	9.363048	10.14028878	2.66801576
	$f_1 = \int_0^T \lvert\dot{u} - \ddot{\bar{u}}\rvert dt$	$f_2 = \int_0^T \lvert s_1\rvert dt$	$f_3 = \int_0^T \lvert s_2\rvert dt$	$f_4 = \int_0^T t s_1^2 dt$	$f_5 = \int_0^T \lvert u\rvert dt$	Feasibility
	22.11604159	86.96316491	1313.96310486	2691.31465381	425.85018165	Yes
NSGAIII	α_1	β_1	δ	μ	γ	k
	3.622405	7.581411	90.17417	3.624616	16.81134	4.338987
	$f_1 = \int_0^T \lvert\dot{u} - \ddot{\bar{u}}\rvert dt$	$f_2 = \int_0^T \lvert s_1\rvert dt$	$f_3 = \int_0^T \lvert s_2\rvert dt$	$f_4 = \int_0^T t s_1^2 dt$	$f_5 = \int_0^T \lvert u\rvert dt$	Feasibility
	5.88461445	102.06520512	**471.50074517**	3016.27999076	**471.50074517**	Yes
OMOPSO	α_1	β_1	δ	μ	γ	k
	96.96229	6.571877	79.655665	1.514812	2.960516	4.32181
	$f_1 = \int_0^T \lvert\dot{u} - \ddot{\bar{u}}\rvert dt$	$f_2 = \int_0^T \lvert s_1\rvert dt$	$f_3 = \int_0^T \lvert s_2\rvert dt$	$f_4 = \int_0^T t s_1^2 dt$	$f_5 = \int_0^T \lvert u\rvert dt$	Feasibility
	24.790992503	**79.3465581**	7312.3628212	**2489.20328043**	943.97872044	Yes

TABLE V. COMPARISON OF DIFFERENT ALGORITHM FOR TUNNING HYPERPARAMETERS OF NONSINGULAR TERMINAL SLIDING MODE CONTROLLER WITH 200 LIMITS FOR FUNCTION EVALUATION

Tuned Hyperparameters of Nonsingular Terminal Sliding Mode Controller with 200 limits for function evaluation						
SMPSO	α_1	β_1	δ	μ	γ	k
	31.231875	6.19709	78.347317	3.931020	43.593004	5.682352
	$f_1 = \int_0^T \lvert\dot{u} - \ddot{\bar{u}}\rvert dt$	$f_2 = \int_0^T \lvert s_1\rvert dt$	$f_3 = \int_0^T \lvert s_2\rvert dt$	$f_4 = \int_0^T t s_1^2 dt$	$f_5 = \int_0^T \lvert u\rvert dt$	Feasibility
	15.220051	91.200026	2525.966872	2632.336478	550.856454	Yes
NSGAII	α_1	β_1	δ	μ	γ	k
	21.256501	3.123190	55.48439	4.19390	17.335351	0.274264
	$f_1 = \int_0^T \lvert\dot{u} - \ddot{\bar{u}}\rvert dt$	$f_2 = \int_0^T \lvert s_1\rvert dt$	$f_3 = \int_0^T \lvert s_2\rvert dt$	$f_4 = \int_0^T t s_1^2 dt$	$f_5 = \int_0^T \lvert u\rvert dt$	Feasibility
	12.852026	**84.540505**	1136.86486775	**2594.73811511**	520.40654534	Yes
NSGAIII	α_1	β_1	δ	μ	γ	k
	4.243728	4.7943222	98.806804	2.868692	37.545664	2.215079
	$f_1 = \int_0^T \lvert\dot{u} - \ddot{\bar{u}}\rvert dt$	$f_2 = \int_0^T \lvert s_1\rvert dt$	$f_3 = \int_0^T \lvert s_2\rvert dt$	$f_4 = \int_0^T t s_1^2 dt$	$f_5 = \int_0^T \lvert u\rvert dt$	Feasibility
	5.23471137	115.87156139	**358.95701638**	3317.22308	**197.0117105**	Yes
OMOPSO	α_1	β_1	δ	μ	γ	k
	89.556200	5.633856	98.787780	10.	83.991619	3.318196
	$f_1 = \int_0^T \lvert\dot{u} - \ddot{\bar{u}}\rvert dt$	$f_2 = \int_0^T \lvert s_1\rvert dt$	$f_3 = \int_0^T \lvert s_2\rvert dt$	$f_4 = \int_0^T t s_1^2 dt$	$f_5 = \int_0^T \lvert u\rvert dt$	Feasibility
	15.22005123	91.20002608	2525.96687235	2632.33647888	550.85645428	Yes

TABLE VI. COMPARISON OF DIFFERENT ALGORITHM FOR TUNNING HYPERPARAMETERS OF NONSINGULAR TERMINAL SLIDING MODE CONTROLLER WITH 500 LIMITS FOR FUNCTION EVALUATION

Tuned Hyperparameters of Nonsingular Terminal Sliding Mode Controller with 500 limits for function evaluation						
SMPSO	α_1	β_1	δ	μ	γ	k
	69.81666	9.935067	69.81666	6.265627	69.81666	7.99692
	$f_1 = \int_0^T \lvert \dot{u} - \ddot{\bar{u}} \rvert dt$	$f_2 = \int_0^T \lvert s_1 \rvert dt$	$f_3 = \int_0^T \lvert s_2 \rvert dt$	$f_4 = \int_0^T t s_1^2 dt$	$f_5 = \int_0^T \lvert u \rvert dt$	Feasibility
	15.17202293	92.71826475	15.17202293	2751.80613499	15.17202293	Yes
NSGAII	α_1	β_1	δ	μ	γ	k
	13.277262	5.04240	13.277262	9.363048	13.277262	2.66801576
	$f_1 = \int_0^T \lvert \dot{u} - \ddot{\bar{u}} \rvert dt$	$f_2 = \int_0^T \lvert s_1 \rvert dt$	$f_3 = \int_0^T \lvert s_2 \rvert dt$	$f_4 = \int_0^T t s_1^2 dt$	$f_5 = \int_0^T \lvert u \rvert dt$	Feasibility
	7.73112307	86.96316491	**7.73112307**	2691.31465381	**7.73112307**	Yes
NSGAIII	α_1	β_1	δ	μ	γ	k
	5.589731	7.581411	5.589731	3.624616	5.589731	4.338987
	$f_1 = \int_0^T \lvert \dot{u} - \ddot{\bar{u}} \rvert dt$	$f_2 = \int_0^T \lvert s_1 \rvert dt$	$f_3 = \int_0^T \lvert s_2 \rvert dt$	$f_4 = \int_0^T t s_1^2 dt$	$f_5 = \int_0^T \lvert u \rvert dt$	Feasibility
	11.91883822	102.06520512	11.91883822	3016.27999076	11.91883822	Yes
OMOPSO	α_1	β_1	δ	μ	γ	k
	96.75430	6.571877	96.75430	1.514812	96.75430	4.32181
	$f_1 = \int_0^T \lvert \dot{u} - \ddot{\bar{u}} \rvert dt$	$f_2 = \int_0^T \lvert s_1 \rvert dt$	$f_3 = \int_0^T \lvert s_2 \rvert dt$	$f_4 = \int_0^T t s_1^2 dt$	$f_5 = \int_0^T \lvert u \rvert dt$	Feasibility
	19.29056043	**79.3465581**	19.29056043	**2489.20328043**	19.29056043	Yes

V. CONCLUSION

In this study, a comparison of four benchmarking optimization algorithms including SMPSO, NSGA-II, NSGA-III, and OMOPSO is presented for tuning hyperparameters of the terminal sliding mode controller. This article aims to reduce the chattering phenomenon and find the optimal hyperparameters of the terminal sliding mode controller. Then the best-optimized hyperparameters of each schema are shown and the objective functions of each algorithm are included. Based on the simulation, it can be concluded that NSGA-II and NSGA-III have better performance. However, when the limitation maximum number of function evaluations is strict, it would be better to use NSGA-III, but if the execution time is more important, it would be better to use NSGA-II, because this algorithm can find the best hyperparameters faster than the other algorithms.

REFERENCES

[1] A. Rodríguez-Molina, E. Mezura-Montes, M. G. Villarreal-Cervantes, and M. Aldape-Pérez, "Multi-objective meta-heuristic optimization in intelligent control: A survey on the controller tuning problem," *Appl. Soft Comput.*, vol. 93, p. 106342, Aug. 2020, doi: 10.1016/j.asoc.2020.106342.

[2] K. Janprom, W. Permpoonsinsup, and S. Wangnipparnto, "Intelligent Tuning of PID Using Metaheuristic Optimization for Temperature and Relative Humidity Control of Comfortable Rooms," *J. Control Sci. Eng.*, vol. 2020, p. e2596549, Jan. 2020, doi: 10.1155/2020/2596549.

[3] L. Chaib, A. Choucha, and S. Arif, "Optimal design and tuning of novel fractional order PID power system stabilizer using a new metaheuristic Bat algorithm," *Ain Shams Eng. J.*, vol. 8, no. 2, pp. 113–125, Jun. 2017, doi: 10.1016/j.asej.2015.08.003.

[4] O. Roeva and T. Slavov, "PID Controller Tuning based on Metaheuristic Algorithms for Bioprocess Control," *Biotechnol. Biotechnol. Equip.*, vol. 26, no. 5, pp. 3267–3277, Jan. 2012, doi: 10.5504/BBEQ.2012.0065.

[5] "Control of fully actuated ocean surface vessels using a class of feedforward approximators | IEEE Journals & Magazine | IEEE Xplore." https://ieeexplore.ieee.org/document/1645126 (accessed Apr. 16, 2022).

[6] "Fast terminal sliding-mode control design for nonlinear dynamical systems | IEEE Journals & Magazine | IEEE Xplore." https://ieeexplore.ieee.org/document/983876 (accessed Apr. 16, 2022).

[7] "An adaptive chattering-free PID sliding mode control based on dynamic sliding manifolds for a class of uncertain nonlinear systems | SpringerLink." https://link.springer.com/article/10.1007/s11071-015-2137-7 (accessed Apr. 08, 2022).

[8] C. Napole, O. Barambones, M. Derbeli, and I. Calvo, "Advanced Trajectory Control for Piezoelectric Actuators Based on Robust Control Combined with Artificial Neural Networks," *Appl. Sci.*, vol. 11, no. 16, Art. no. 16, Jan. 2021, doi: 10.3390/app11167390.

[9] "Design and performance analysis of PID controller for an automatic voltage regulator system using simplified particle swarm optimization | Elsevier Enhanced Reader." https://reader.elsevier.com/reader/sd/pii/S0016003212001573?token=2287137CADC45FCAFAFBA0A7B25E63161DBDF1ED3FDB43E22FF218BDE14A6718D24EDFC7AF2C4D71D1926E9EF7BB

F356&originRegion=us-east-1&originCreation=20220409005840 (accessed Apr. 08, 2022).

[10] W.-D. Chang and C.-Y. Chen, "PID Controller Design for MIMO Processes Using Improved Particle Swarm Optimization," *Circuits Syst. Signal Process.*, vol. 33, no. 5, pp. 1473–1490, May 2014, doi: 10.1007/s00034-013-9710-4.

[11] D. Brockhoff and T. Tušar, "Benchmarking algorithms from the platypus framework on the biobjective bbob-biobj testbed," in *Proceedings of the Genetic and Evolutionary Computation Conference Companion*, Prague Czech Republic, Jul. 2019, pp. 1905–1911. doi: 10.1145/3319619.3326896.

[12] "An Evolutionary Many-Objective Optimization Algorithm Using Reference-Point-Based Nondominated Sorting Approach, Part I: Solving Problems With Box Constraints | IEEE Journals & Magazine | IEEE Xplore." https://ieeexplore.ieee.org/document/6600851 (accessed Apr. 16, 2022).

[13] "A fast and elitist multiobjective genetic algorithm: NSGA-II | IEEE Journals & Magazine | IEEE Xplore." https://ieeexplore.ieee.org/document/996017 (accessed Apr. 16, 2022).

[14] M. R. Sierra and C. A. Coello Coello, "Improving PSO-Based Multi-objective Optimization Using Crowding, Mutation and ∈-Dominance," in *Evolutionary Multi-Criterion Optimization*, Berlin, Heidelberg, 2005, pp. 505–519. doi: 10.1007/978-3-540-31880-4_35.

[15] "SMPSO: A new PSO-based metaheuristic for multi-objective optimization | IEEE Conference Publication | IEEE Xplore." https://ieeexplore.ieee.org/document/4938830 (accessed Apr. 16, 2022).

[16] "The particle swarm - explosion, stability, and convergence in a multidimensional complex space | IEEE Journals & Magazine | IEEE Xplore." https://ieeexplore.ieee.org/document/985692 (accessed Apr. 17, 2022).

[17] M. Roozegar, M. Ayati, and M. J. Mahjoob, "Mathematical modelling and control of a nonholonomic spherical robot on a variable-slope inclined plane using terminal sliding mode control," *Nonlinear Dyn.*, vol. 90, no. 2, pp. 971–981, Oct. 2017, doi: 10.1007/s11071-017-3705-9.